JOURNAL OF MATERIALS SCIENCE 32 (1997) 1177–1185

Filler–matrix debonding in glass bead-filled polystyrene

A. MEDDAD, B. FISA
Centre de recherche appliquée sur les polymères (CRASP), École Polytechnique de Montréal, Canada

The debonding process in a glassy polymer filled with glass beads during constant strain rate tensile loading has been analysed both theoretically and experimentally. A model which combines concepts of damage mechanics and the time dependence of interfacial strength has been proposed and compared with experimental results on glass bead-filled polystyrene. The stress–strain behaviour and the debonding could be modelled using a Bartenev-type relation for the destruction of the interfacial bond and by considering the gradual transformation on the initially well-bonded composite into foam. A good agreement between calculated and experimental data was achieved.

Nomenclature

A_1	Constant, Kerner–Lewis equation (Equation 3)
B	Debonding rate exponential constant (Equation 7)
B_1, B_2	Constants, Kerner–Lewis equation (Equations 3 and 4)
d	Filler particle diameter
E_f, E_m	Filler and matrix modulus
E_0	Initial modulus of composite
E_c	Secant modulus of composite
E'_c	Value of composite modulus used to calculate effective stress, $\bar{\sigma}$ (Equation 8)
E_1, E_2	Relative moduli of the filled and debonded composite (Equations 4 and 5)
K	Proportional constant of debonding rate
t	Time (independent variable)
t_f	Time of failure (Equation 6)
ε, ε_t	Axial and transverse strain
ε_b	Strain at break of composite
ε_d	Strain at which debonding occurs
Δl	Displacement recorded by extensometer
ϕ, ϕ_b, ϕ_d	Filler volume fraction, overall (ϕ), bonded (ϕ_b) and debonded (ϕ_d)
ϕ_m	Maximum packing fraction (Equation 4)
ν, ν_0	Poisson ratio and initial Poisson ratio
σ, $\bar{\sigma}$, σ_b	Applied stress, effective stress and stress at break
ζ, ζ_d	Volume strain and volume strain due to debonding

1. Introduction

The mechanical behaviour of multiphase materials, such as filled and reinforced plastics or polymer blends, is closely related to the degree of interfacial adhesion between their various components. We have all seen micrographs of fracture surfaces from which "good" or "poor" adhesion is qualitatively evaluated. A more ambitious approach aims to develop methods which can follow the onset and development of damage as it occurs during mechanical loading. One of the more straightforward techniques is tensile dilatometry (recently reviewed by Naqui and Robinson [1]). In this method, the volume strain, ζ, calculated using axial and transverse strains, ε and ε_t, respectively

$$\zeta = (1 + \varepsilon)(1 - \varepsilon_t)^2 - 1 \quad (1)$$

is compared to the dilational response of the material which is obtained from the low strain value of the Poisson ratio, ν_0 (Fig. 1). The point at which the experimental ζ versus ε curve departs from the dilational response is an indication that the deformation mechanism has changed. Cavitation mechanisms such as debonding (or crazing) lead to an increase of volume strain with ε compared to dilation. When the volume strain increases at a rate slower than dilation, the material is said to exhibit deviatoric behaviour – a consequence of mechanisms such as shear yielding. A number of authors have interpreted the mechanical behaviour of filled polymers with the help of tensile dilatometry [2–4] but the conclusions drawn from the results are often contradictory. Using another approach, Vollenberg *et al.* [5], working with glass bead-filled plastics, attributed a section of the tensile stress, σ, versus axial strain, ε, curve to the debonding process (see Fig. 2). In this case the first elastic stage (part 1), which corresponds to the deformation of well-bonded composite, is followed by the onset and the progression of debonding (part 2). The last stage (part 3) is attributed to processes such as crazing or shear yielding.

In general, the effect of adding a second rigid phase to polymers is to enhance the elastic (short-term, small-strain) stiffness substantially, but the effect on other properties is more complex to analyse. This is

0022–2461

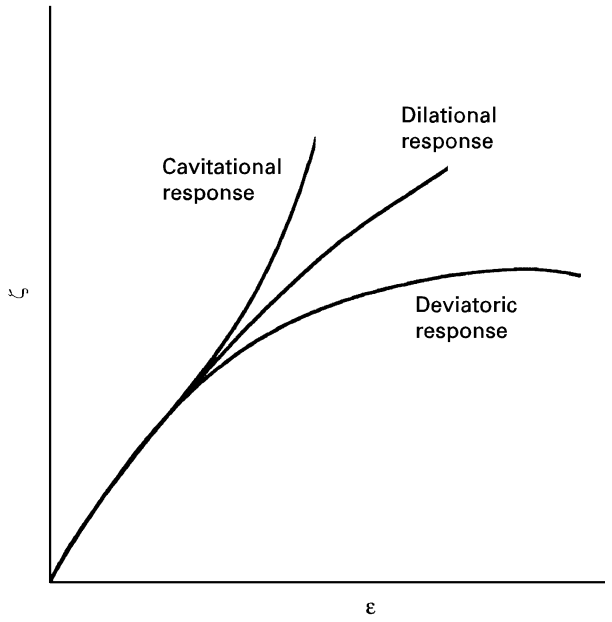

Figure 1 Volume strain, ζ, as function of axial strain, ε (after Naqui and Robinson [1]).

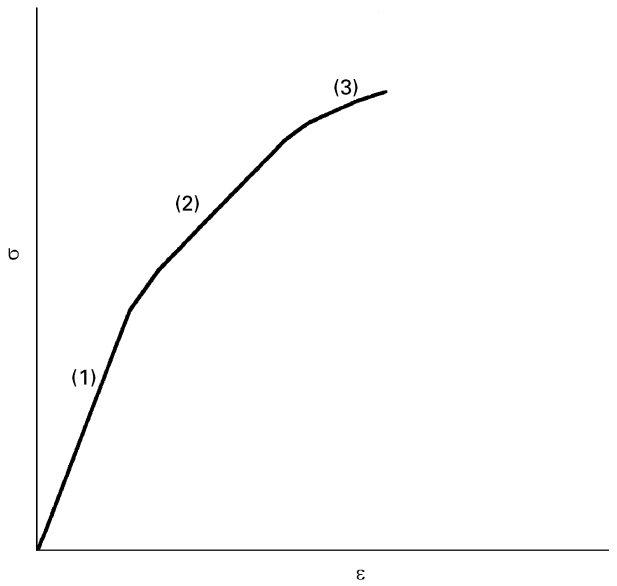

Figure 2 Different stages in a stress–strain behaviour of filled polymers: (1) elastic, (2) debonding, (3) crazing and/or shear yielding (after Vollenberg *et al.* [5]).

because, as a result of straining, the material properties change because of damage related to factors such as filler/matrix debonding, but also due to the viscoelastic nature of the matrix. A number of studies have been performed to evaluate the debonding resulting from the tensile loading. Newaz and Walsh [9] studied it in sand and fly ash-filled epoxy resins. Using the loading and unloading test, they showed that the debonding process can be interpreted in terms of damage mechanics. However, because only the rigid phase (the filler) is excluded from the load bearing as the debonding progresses, the material loses its stiffness not only from the reduction of the effective section but also from a reduction of the effective filler concentration in the remaining material. The model developed by Anderson and Farris [10–12], which was applied to a filled polyurethane elastomer, calculates the non-linear stress–strain behaviour using an energy balance. Their model has been used to predict the loss of stiffness assuming separately either a reduction of the effective filler concentration or an addition of voids, both resulting from debonding. Volodin *et al.* [13] have suggested that the stress and strain of filled polymers can be described with the help of two parameters which depend on the volume fraction of the filler, its particle shape and its interaction with the matrix. Recently, a mathematical model developed from the tensile stress–axial strain and from the volume strain–axial strain data has been proposed by Zezin [14]. It describes the damage accumulation in terms of debonded filler fraction. The micromechanical model proposed by Ravichandran and Liu [15] considers the debonding-induced damage as an isotropic function depending on an internal variable. The theory developed by Zhao and Weng [16] to describe the debonding process in a ductile composite containing aligned oblate inclusions, uses a statistical function to model the breakage of filler/matrix bonds. Other authors have focused their studies on the modelling of the stress distribution in filled polymers using finite element analysis and on their fracture behaviour [17, 18]. Their results show the dependence of the debonding stress on the filler/matrix interaction.

Despite a large body of literature on the mechanical behaviour of filled polymers, most of the technological data generated by and used in the industry is in the form of properties such as yield or breaking stress and elongation from the constant strain-rate tests. It would certainly be desirable if this simple, most widely-used mechanical test could also be used to detect the onset and to follow the progression of filler/matrix debonding (or of the other damage process induced by the presence of a second phase in the matrix). The objective of this work is to examine if and how this information can be extracted from the tensile stress–strain data of an elastic matrix filled with rigid spherical inclusions. The debonding process is analysed theoretically – the material model takes into account the gradual loss of stiffness caused both by the filler matrix debonding and by the decrease of the effective filler concentration in the material. The results are compared with experimental stress–strain data of glass bead-filled polystyrene.

2. Experimental procedure

The polymer used in this study is an injection-grade polystyrene (PS) of granular form (Dylark 232 from ARCO Chemical Company, Scarborough, Ontario, Canada). Glass beads (untreated and silane treated), obtained from Potters Ballotini, were used as fillers. The average bead diameter was about 45 μm. The following compositions were moulded: 0, 5, 10, 20 and 40 vol % corresponding to 0, 11, 21, 38 and 62 wt %. The PS and glass were first compounded on a twin-screw extruder before being injection moulded. The compounding and injection-moulding conditions were those recommended by the resin supplier. The

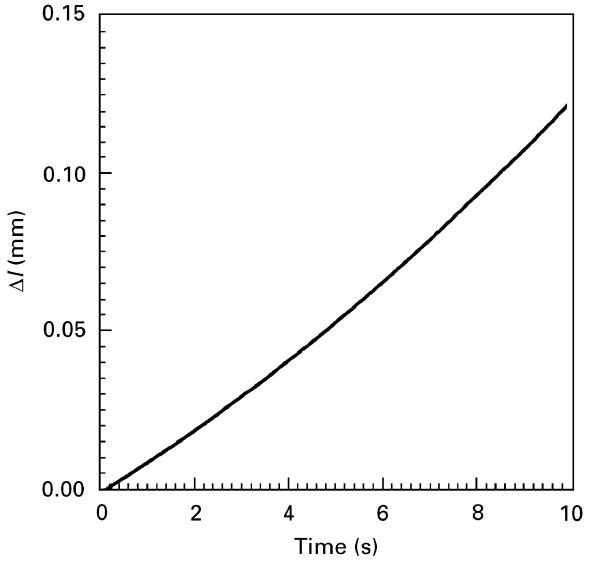

Figure 3 Typical variation between crosshead strain and extensometer recorded strain as a function of time (PS + 20 vol% untreated glass beads).

3 mm deep mould cavity had the ASTM D638-type I tensile bar shape. A tensile testing machine with crosshead speed of 5 mm min^{-1} (this corresponds to about 0.12% s^{-1} strain rate) was used at 23 °C and 50% relative humidity. The strain data were collected using two extensometers: an MTS 638.13C axial extensometer (gauge length 10 mm) and an Instron Model 6048.007 transverse extensometer (variable gauge length). The strains and the stress were recorded simultaneously on a PC using a data acquisition software at a frequency of 10 points/s. Fig. 3 shows the actual gauge length of the increase, Δl, recorded by the axial extensometer, as a function of time for 20 vol % composite. The strain is nearly proportional to the crosshead displacement.

3. Experimental results

The results are summarized in Table I and Fig. 4 shows the stress–strain curves of PS containing between 0 and 40 vol % glass beads. The initial modulus, E_0, depends only on the glass content (it is independent of the silane treatment). When Young's modulus is calculated using the Kerner–Lewis equation (see Equation 3 below) [19], the calculated values are in agreement with the experimental values. A "conventional" cursory interpretation of the stress–strain curves would attribute the departure of the "untreated" (NT) curve from its "treated" (T) counterpart to an earlier onset of debonding (example for 20 vol %; at $\sigma \simeq 20$ MPa and $\varepsilon \simeq 0.5\%$). Alternatively, the debonding in the treated composite may be said to begin at a higher stress. Our results show that both the stress and strain at which the deviation from linearity occurs depend on the filler content – this finding appears to be at variance with those reported by Dekkers [6] who found that the strain at which the deviation starts is independent of filler content. The stress at break is also lower for untreated rather than treated glass beads. As far as the ζ versus ε function is

TABLE I Tensile properties of PS/glass bead composites

ϕ	E_0 (GPa)			ε_b (%) at break		σ_b (MPa) at break		ν_0	
	T	NT	Calculated[a]	T	NT	T	NT	T	NT
0			2.84		1.8		44		0.31
0.05	3.14	3.11	3.13	2.40	2.0	50	46	0.29	0.29
0.10	3.50	3.47	3.47	2.10	1.70	48	41	0.28	0.28
0.20	4.38	4.33	4.36	1.45	1.20	44	37	0.27	0.27
0.40	7.75	7.70	7.90	0.65	0.63	38	37	0.26	0.26

[a] Using Equation 3 with $\phi_d = 0$, $\nu = 0.31$, $A_1 = 1.11$, $B_1 = 0.92$ and $\phi_m = 0.64$.

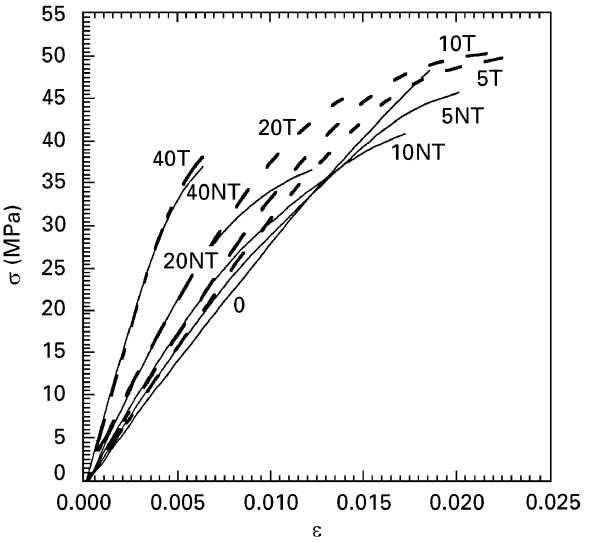

Figure 4 Tensile stress–strain curves, σ versus ε of filled PS. (– –) Treated; (——) untreated glass beads. Numbers on curves denote the glass concentration (vol %).

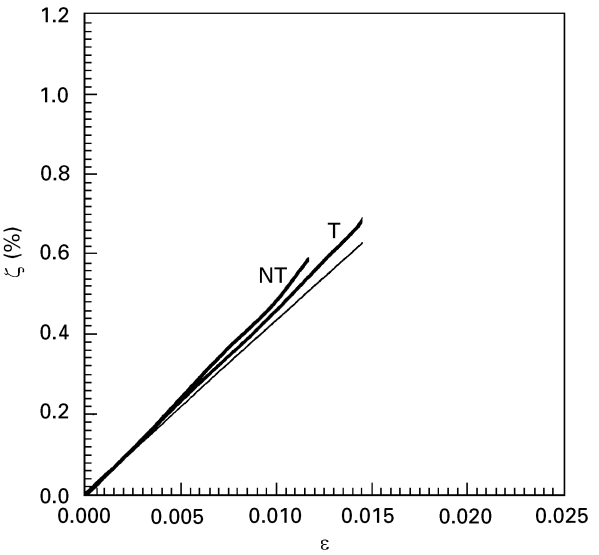

Figure 5 Volume strain, ζ, versus nominal strain, ε, of PS filled with 20 vol % glass beads. (20T) treated; (20NT) untreated glass. (——) Dilational behaviour of filled PS.

concerned, the comparison between the filled and the unfilled polymer shows a decrease in the initial value of the Poisson ratio, ν_0 (Table I) with increasing glass content. The values found are in agreement with those predicted by Chow's model [20]. Fig. 5 shows the

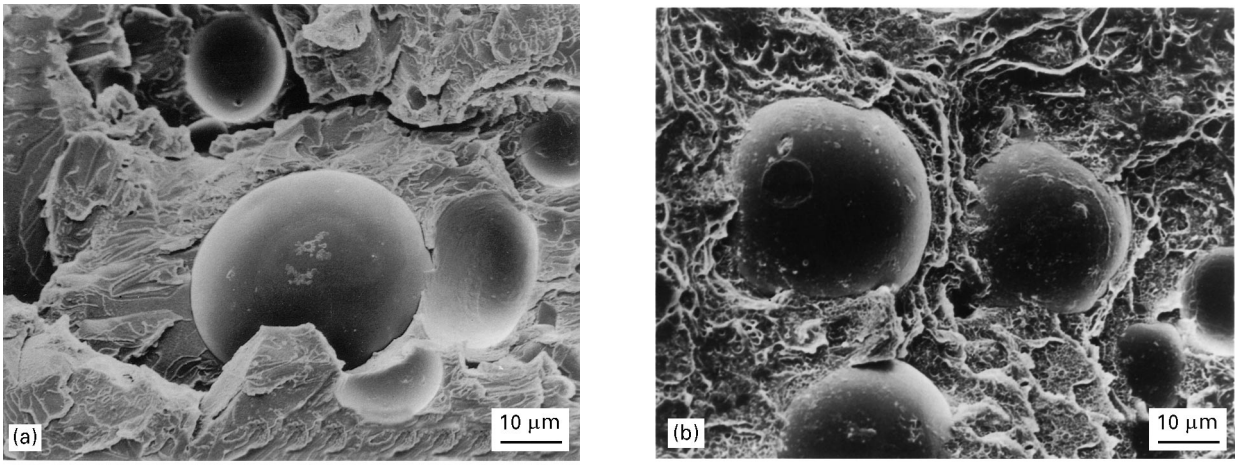

Figure 6 Scanning electron micrographs of PS + 10 vol % glass beads; (a) untreated; (b) silane treated.

ζ versus ε function of the 20 vol % filled PS in the range of strains of $\varepsilon \leqslant 1.5\%$. The differences between the measured volume strain and that calculated using a low-strain Poisson ratio of $\nu_0 = 0.27$, are very small and cannot be used accurately to detect the onset of debonding. This suggests that the dilatometry is more useful for materials able to withstand larger strains.

Scanning electron micrographs of surfaces taken following tensile fracture (Fig. 6) clearly show that the debonding process occurred, although it would be difficult to infer any differences in the degree of interfacial adhesion between the treated and untreated beads.

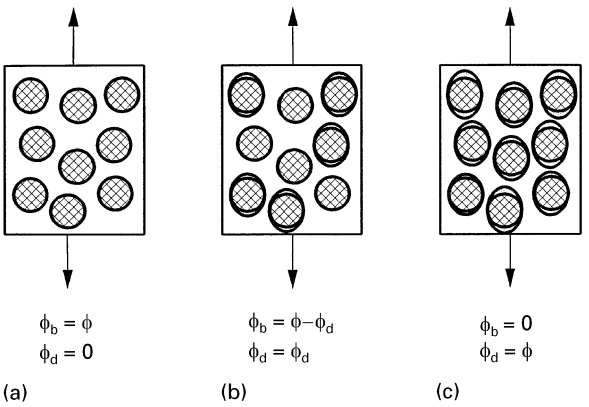

Figure 7 Schematic representation of a filled polymer subjected to uniaxial tension. (a) Well-bonded composite, (b) partially debonded composite, and (c) fully debonded composite.

4. The model

The model is based on the following assumptions (see Fig. 7).

1. Initially, all filler particles (volume fraction, ϕ) are well bonded to the matrix (bonded filler volume fraction $\phi_b = \phi$, Fig. 7a). The material behaviour can be described by the Kerner–Lewis equation (see below).

2. Upon straining, the filler particles become progressively debonded ($\phi_b = \phi - \phi_d$, ϕ_d being the debonded filler volume fraction). The debonded particles do not bear any load (Fig. 7b).

3. The completely debonded composite ($\phi_b = 0$, $\phi_d = \phi$) behaves as a foam containing a volume fraction of voids equal to ϕ_d (Fig. 7c). Its behaviour can also be described by the Kerner–Lewis equation.

4. The debonding rate ($d\phi_d/dt$) depends on the applied stress and the number of particles available for debonding ($\phi - \phi_d$).

During the constant strain-rate tensile test ($d\varepsilon/dt = \text{const}$), the applied stress, σ, follows the relation

$$\frac{d\sigma}{dt} = \frac{d(E_c\,\varepsilon)}{dt} = \varepsilon\left(\frac{dE_c}{dt}\right) + E_c\left(\frac{d\varepsilon}{dt}\right) \qquad (2)$$

where E_c is the secant modulus of the composite. The modulus, E_c, decreases as debonding progresses. The partially debonded composite containing a volume fraction, ϕ, of the filler (of which ϕ_d is debonded: $0 \leqslant \phi_d \leqslant \phi$) is considered to consist of three components: (i) matrix (modulus E_m), (ii) bonded filler (volume fraction $[\phi - \phi_d]$, modulus E_f), and (iii) debonded filler (each vacuole containing a debonded filler particle behaves as a void). The modulus of such hybrid material can be described by the Kerner–Lewis equation [19]

$$E_c = E_m\ E_1\ E_2 \qquad (3)$$

where E_1 represents the relative modulus of the still bonded-filled material

$$E_1 = \frac{1 + A_1\ B_1\ (\phi - \phi_d)}{1 - B_1\ \ \psi(\phi - \phi_d)} \qquad (4)$$

with $A_1 = (7 - 5\nu)/(8 - 10\nu)$, $B_1 = (E_f/E_m - 1)/(E_f/E_m + A_1)$ and $\psi = 1 + \phi(1 - \phi_m)/\phi_m^2$, ν is the Poisson ratio of the matrix, ψ is a "crowding factor" which depends on ϕ_m (the maximum packing fraction of the filler). The modulus, E_2, is the relative modulus of the foam with a void fraction equal to ϕ_d. E_2 is then given by

$$E_2 = \frac{1 - \phi_d}{1 - B_2\ \psi\ \phi_d} \qquad (5)$$

with $B_2 = -1/A_1$. It is worth noting that the Kerner–Lewis equation and other expressions of this type have been successfully applied to hybrid materials [21] and to high-density foams [22].

Considering the heterogeneous nature of materials under consideration it seems reasonable to adapt Bartenev's equation [23, 24] for time to failure, t_f, of a material subjected to an effective stress, $\bar{\sigma}$. This equation, originally developed for materials containing defects, is written here in simplified form

$$t_f = \frac{\exp(-B\ \bar{\sigma})}{K\ \bar{\sigma}} \tag{6}$$

The constants B and K depend on the temperature, the material molecular structure, and the nature and number of defects. It should be noted that this and other equations (e.g. Zhurkov–Bueche [25]) relating the time to failure to the applied stress have a theoretical basis and are often considered as interpolation formulas of a semi-empirical nature – useful for the mathematical expression of experimental data. Applying the Bartenev concept to a filled material, we assume that the time to failure of the filler/matrix interface can be described by Equation 6. The probability of debonding is proportional to $1/t_f$. The debonding rate, $d\phi_d/dt$, is then considered to be proportional to $K\bar{\sigma}\exp(B\bar{\sigma})$ (the constants K and B are related to the overall behaviour of the filled material rather than only to that of single particle/matrix interface, $\bar{\sigma}$ is the effective stress – see below) and to $(\phi - \phi_d)$

$$\frac{d\phi_d}{dt} = (\phi - \phi_d)\ K\ \bar{\sigma}\exp(B\ \bar{\sigma}) \tag{7}$$

The effective stress, $\bar{\sigma}$, which acts only on the matrix and on the still-bonded filler, can be related to the measured stress, σ (which is calculated using the entire sample cross-section, including its debonded portion), using the strain equivalence principle [26]. A material containing a filler fraction $(\phi - \phi_d)$ but no voids will have a modulus E_c'

$$E_c' = E_m\ E_1 \tag{8}$$

According to the strain equivalence principle

$$\varepsilon = \frac{\bar{\sigma}}{E_c'} = \frac{\sigma}{E_c} \tag{9}$$

This leads to

$$\bar{\sigma} = \frac{\sigma}{E_2} \tag{10}$$

Because

$$\frac{dE_c}{dt} = \frac{dE_c}{d\phi_d}\left(\frac{d\phi_d}{dt}\right) \tag{11}$$

a simultaneous solution of Equations 2 and 7 can be obtained using known values of E_m, $d\varepsilon/dt$ and ϕ, and using Equations 3–5, 10 and 11.

Solution of Equations 2 and 7 using the fourth-order Runge Kutta method, yields the value of the secant modulus, E_c, and of the debonded fraction, ϕ_d. To determine the appropriate values of K and B, the calculated results are compared, with the help of the Marquardth–Levenberg algorithm, to the values of ϕ_d computed from the experimental stress–strain data using Equation 3.

The volume increase due to debonding, ζ_d, can also be calculated assuming, for example, that each void created by debonding of a spherical particle (diameter d) is an ellipsoid with its two shorter axes equal to d and its longer axis equal to $d\ [1 + (\varepsilon - \varepsilon_d)]$, where ε_d represents the strain at which the particle becomes debonded [14]. It follows that

$$\zeta_d = \int_0^{\varepsilon} \phi_d\ d\varepsilon \tag{12}$$

5. Results and discussion

Two extreme cases of stress–strain curves of a composite material, calculated using properties of polystyrene ($E_m = 2.84$ GPa, $\nu_0 = 0.31$) and glass beads ($E_f = 72$ GPa, $\nu = 0.25$) with $\phi = 0.2$ and $d\varepsilon/dt = 1.22 \times 10^{-3}\ s^{-1}$ are shown in Fig. 8. When $B \to 0$, the debonding rate is proportional to the effective stress, $\bar{\sigma}$. The measured stress σ versus ε function (curve 5) starts to deviate from linearity at relatively low strains and moves to the completely debonded material (line 3) over a broad range of strains. When B is very large, all the debonding occurs at a nearly constant effective stress, $\bar{\sigma}$ (curve 4, calculated using $K = 2.9 \times 10^{-20}$ $MPa^{-1}\,s^{-1}$ and $B = 4\ MPa^{-1}$). The material then exhibits what in σ versus ε presentation appears as a yield – the measured stress, σ, decreases as the material approaches the fully debonded state.

The corresponding ϕ_d versus ε and ϕ_d versus $\bar{\sigma}$ curves are shown in Fig. 9. The shapes of these curves suggest that the Bartenev-type equation can cover the range of situations likely to be found in

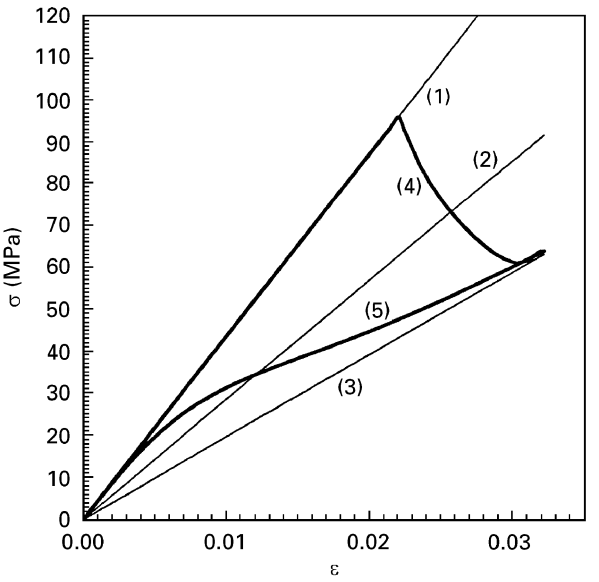

Figure 8 Stress–strain curves calculated using Equations 2 and 7, with $\phi = 0.2$ and $E_m = \text{const} = 2.84$ GPa (see text): (1) Bonded composite ($K = 0$); (2) matrix; (3) fully debonded composite ($K \to \infty$); (4, 5) limiting cases when all debonding occurs at constant effective stress $\bar{\sigma}$ ($K \to 0$, $B \to \infty$; curve 4) and when the debonding rate is proportional to $\bar{\sigma}$ ($B = 0$; curve 5).

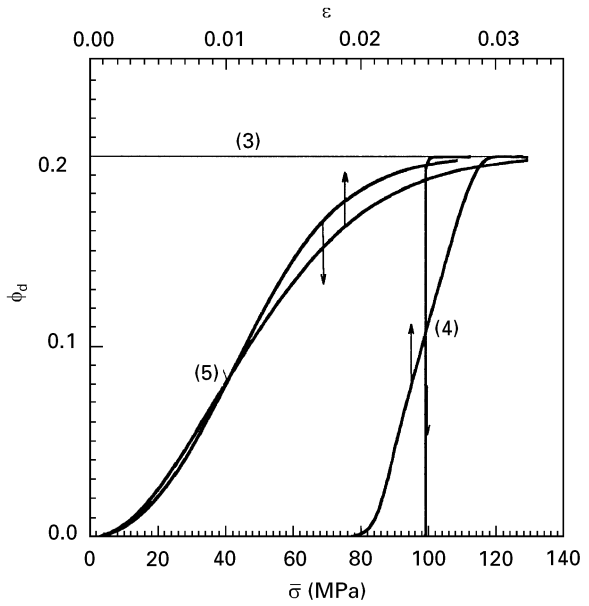

Figure 9 Debonded filler fraction, ϕ_d, as a function of effective stress, $\bar{\sigma}$, and as a function of strain, ε, calculated using Equations 2 and 10. The curves are numbered as in Fig. 8.

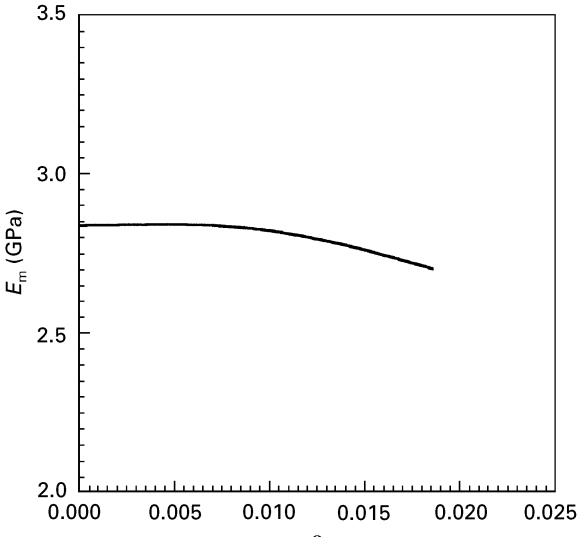

Figure 10 Secant modulus of neat PS as a function of strain.

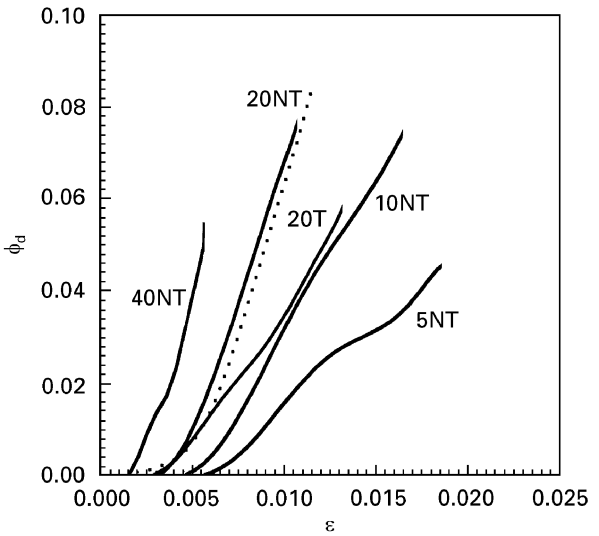

Figure 11 Volume fraction of debonded glass beads, ϕ_d, as a function of strain, ε, for different glass concentrations; calculated from experimental data of the matrix and of composites using Equation 2. (. . .) Calculated using a constant value of $E_m = 2.84$ GPa.

multiphase materials. In a perfectly uniform, ordered composite the debonding might indeed occur at a constant effective stress (case 4, $K \to 0$, $B \to \infty$). In a real material, in which the dispersed phase distribution is at best uniformly random, the particles are of different sizes and shapes, and local stress fluctuations are caused not only by the material inherent heterogeneities but also by residual stresses which vary throughout the thickness, the debonding will obviously occur over a broader range of stress and strain. The question is whether, in most "real" materials, the debonding process (or other type of damage) can be described by curves situated between the extreme cases of curves 4 and 5 in Figs 8 and 9.

Before considering the applicability of the proposed model, let us evaluate the debonding process with the help of Equation 3. The solution of Equation 3 makes it possible to calculate the volume fraction of the debonded filler, ϕ_d, using the experimentally determined values of E_c and E_m. Fig. 10 shows the secant modulus, E_m, of neat PS as a function of strain. Beyond 0.95%, a slow decrease in secant modulus is recorded. This shows that the matrix is not elastic over the whole range of strains studied (Fig. 4). For example, at 0.5%, 1.5% and 2%, the experimental values of E_m are 2.84, 2.77 and 2.68 GPa, respectively. The curves in Fig. 11 show the volume fraction of debonded filler, ϕ_d, calculated from Equation 3 when E_m is taken as a constant (full line) and from experimental stress–strain data of the matrix (dotted line, for $\phi = 0.2$). Because the error induced by an assumption of constant matrix modulus is small, all calculations shown below were made with the $E_m = \text{const.} = 2.84$ GPa.

The following comments concerning the concentration dependence of the debonded filler fraction can be made.

(a) The strain, ε, at which the debonding appears, decreases with increasing filler concentration. This has been attributed to the thermal stress resulting from the differences of the matrix and filler thermal expansion coefficients. This thermal stress, which tends to shrink the matrix around the filler as the composite is cooled from the moulding temperature, decreases with increasing filler content [5]. The debonding process is also related to the area occupied by the filler. The calculated stress distribution around a filler changes with filler content [17].

(b) At $\phi = 0.05$, the volume fraction of debonded filler, ϕ_d, shows a certain plateau at a strain $\varepsilon \simeq 1.2\%$. This corresponds to a point when about half of the beads have debonded. Because the materials used here were all made by the injection-moulding process, most material properties exhibit significant variations throughout the thickness due to phenomena such as matrix orientation, residual stress, etc. [27]. In glassy polymers, in particular, the properties

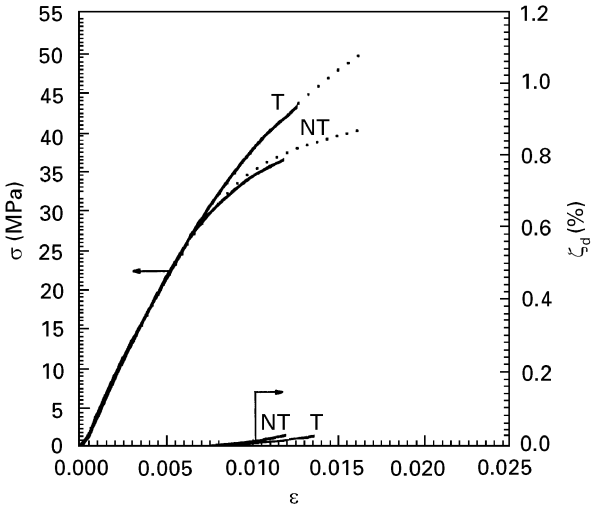

Figure 12 (. . .) Calculated and (——) experimental stress–strain curves of filled PS. Debonded volume, ζ_d, was calculated using Equation 12.

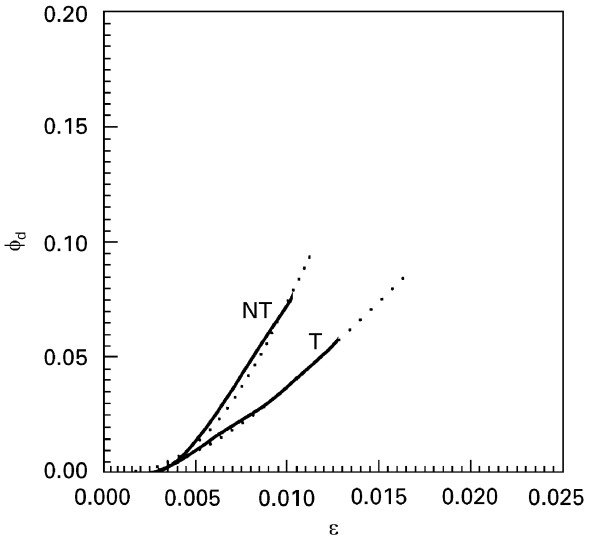

Figure 13 Debonded filler fraction, ϕ_d, as a function of strain, ε, (——) calculated using Equations 3–5 from experimental σ versus ε data of 20 vol % composites, (. . .) Predicted by the model using values K and B of Table II.

of the highly oriented skin and of the more or less randomly oriented core are known to be very different [28]. It is conceivable that the particular shape of the ϕ_d versus ε curve at $\phi = 0.05$ is related to the layered structure of injection mouldings. For the other concentrations, the samples break well before half of the filler has debonded and before the plateau (if one exists) becomes visible.

(c) One of the interesting results of this work is that the effect of surface treatment on the debonding process is somewhat different from that previously reported. The debonding starts at about the same strain for both materials, treated and untreated (for example, at $\varepsilon \simeq 0.4\%$ when $\phi = 0.2$ vol %) but the rate of debonding ($d\phi_d/d\varepsilon$) is higher in the absence of the coupling agent.

(d) All composites broke before the fully debonded state was reached.

Fig. 12 shows the experimental and calculated data of stress–strain curves of 20 vol % filled PS. Although, as mentioned above, both materials (NT and T) break well before complete debonding (the σ versus ε curves do not even cross the neat PS curve), the experimental stress–strain data can be matched to curves calculated using appropriate values of K and B. They are $K = 0.29 \times 10^{-3}$ MPa^{-1} s^{-1}, $B = 6.22 \times 10^{-2}$ MPa^{-1} for untreated beads composite, and $K = 0.34 \times 10^{-3}$ MPa^{-1} s^{-1}, $B = 3.80 \times 10^{-2}$ MPa^{-1} for the 20 vol % composite made with treated beads. The debonded fraction, ϕ_d, dependence on the strain determined from the experimental data using Equation 3 also corresponds to that calculated from the theoretical model (Fig. 13). The volume strain due to debonding, ζ_d, shown in Fig. 12, calculated using Equation 12, is very small and appears to be of the same order of magnitude as the difference between the measured and dilational behaviours shown in Fig. 5. For other glass concentrations, similar agreement between the predicted and experimental results was obtained.

Optimized values of constants K and B are listed in Table II. The pre-exponential constant K appears to

TABLE II $K\phi$ and B values of polystyrene/glass beads composites (T) treated and (NT) untreated glass

ϕ	$K\phi$ (10^{-4} MPa^{-1} s^{-1})		B (10^{-2} MPa^{-1})	
	T	NT	T	NT
0.05	0.70	0.56	2.78	5.17
0.10	0.69	0.61	3.13	5.80
0.20	0.67	0.59	3.80	6.22
0.40	0.65	0.57	4.13	5.82

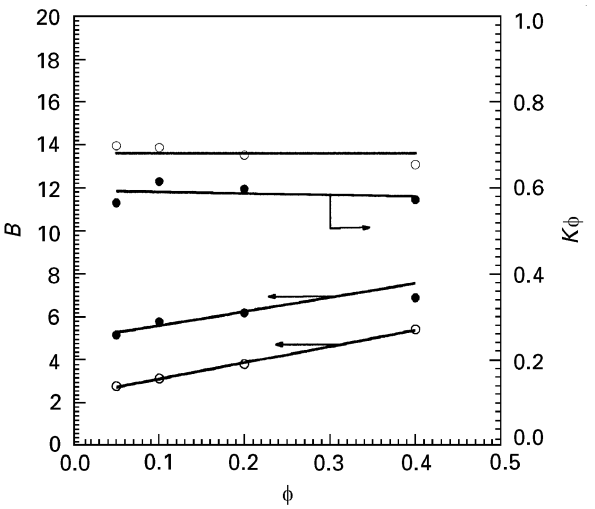

Figure 14 Values of $K\phi$ (10^{-4} MPa^{-1} s^{-1}) and of B (10^{-2} MPa^{-1}) as a function of ϕ. (●) Untreated, (○) treated.

be inversely proportional to ϕ while the value of B increases with the glass concentration (Fig. 14). Because the function ($K\bar{\sigma}\exp B\bar{\sigma}$) really represents a probability that a filler particle embedded in the matrix will debond when the composite is subjected to a stress, $\bar{\sigma}$, it is interesting to consider its dependence on the stress and strain. Fig. 15 shows how $K\bar{\sigma}\exp(B\bar{\sigma})$

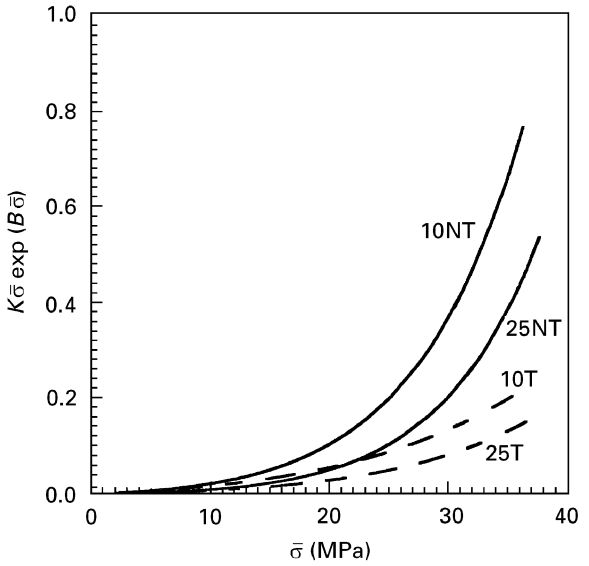

Figure 15 Debonding probability $K\bar{\sigma}\exp(B\bar{\sigma})$ as a function of stress, $\bar{\sigma}$, for $\phi = 0.10$ (treated glass, $K = 0.68 \times 10^{-3}$ MPa^{-1} s^{-1}, $B = 3.11 \times 10^{-2}$ MPa^{-1}; untreated glass, $K = 0.58 \times 10^{-3}$ MPa^{-1} s^{-1}, $B = 5.62 \times 10^{-2}$ MPa^{-1}) and $\phi = 0.25$ (treated glass, $K = 0.27 \times 10^{-3}$ MPa^{-1} s^{-1}, $B = 4.25 \times 10^{-2}$ MPa^{-1}; untreated glass, $K = 0.23 \times 10^{-3}$ MPa^{-1} s^{-1}, $B = 6.61 \times 10^{-2}$ MPa^{-1}).

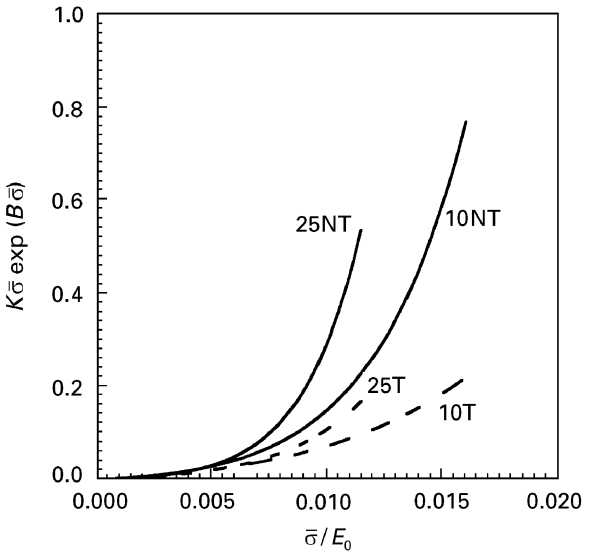

Figure 16 Debonding probability $K\bar{\sigma}\exp(B\bar{\sigma})$ as a function of strain function $(\bar{\sigma}/E_0)$, using the same notation as in Fig. 15.

varies with the stress, $\bar{\sigma}$, for two concentrations of glass beads: 10 and 25 vol % (values of K and B used were extrapolated from Fig. 14). For both concentrations, the effect of silane treatment is important. At a given applied stress, the probability of debonding increases with decreasing filler concentration. This can be attributed to the fact that the stress concentration at the interface is influenced by the magnitude of stiffness differential between the particle and the surrounding material. With a higher filler concentration, this differential is smaller and, at a given value of stress, the local stress at the interface will be lower, leading to a lower probability of debonding. This observation, based on experimental results, is in agreement with the finite element analysis of a composite material containing randomly distributed rigid spherical particles [17]. When the value of $K\bar{\sigma}\exp(B\bar{\sigma})$ is followed as a function of strain, for example by drawing $K\bar{\sigma}\exp(B\bar{\sigma})$ versus $\bar{\sigma}/E_0$ as in Fig. 16, the higher stress required to deform the stiffer, more filled, material predominates and the $K\bar{\sigma}\exp(B\bar{\sigma})$ assumes, at a given strain, a higher value than for a composite containing a smaller amount of filler.

Finally, the results presented so far can be used to validate a simple method for detection of debonding. When the ratio of secant moduli, E_c/E_m, is plotted against the strain ε (Fig. 17), virtually the same conclusions as to the onset and the rate of debonding can be drawn from it as from the more complex treatment that led to the ϕ_d versus ε graphs (shown in Fig. 12). The same approach can be applied to other materials including those made with viscoelastic matrix ($E_m \neq$ const) and/or with non-spherical fillers. The results will be made available shortly.

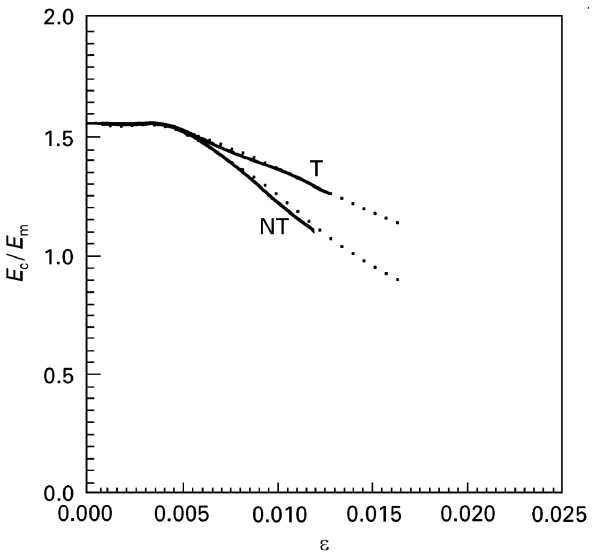

Figure 17 Secant moduli ratio, E_c/E_m, as a function of strain, ε. (——) Experimental and (. . .) calculated from the model.

6. Conclusion

A simple model has been used to describe a particulate composite undergoing a constant strain–rate test. The stress–strain behaviour and the debonding is modelled using a Bartenev-type relation for the destruction of interfacial bonds and by considering the gradual transformation of the initially well-bonded composite into foam. The volume change resulting from debonding is small compared to dilational response. The debonding starts at about the same strain in composite-filled material with a given volume fraction of silane-treated and untreated glass beads, but the rate of debonding is higher in the absence of the coupling agent. A good agreement was achieved between calculated and experimental data. The relative loss of stiffness (E_c/E_m) during the test is directly related to the debonding process.

Acknowledgements

The financial support of NSERC (Natural Sciences and Engineering Research Council of Canada) is gratefully acknowledged.

References

1. S. I. NAQUI and I. M. ROBINSON, *J Mater. Sci.* **28** (1993) 1421.
2. E. A. A. VAN HARTINGSVELDT and J. J. VAN AARTSEN, *Polymer* **30** (1984) 1989.
3. M. E. J. DEKKERS and D. HEIKENS, *J. Mater. Sci.* **30** (1985) 2389.
4. B. PUKANSZKY, M. VAN ES, F. H. J. MAURER and G. VÖRÖS, *ibid.* **29** (1994) 2350.
5. P. VOLLENBERG, D. HEIKENS and H. C. B. LADAN, *Polym. Compos.* **9** (1988) 382.
6. M. E. J. DEKKERS, Doctorate Thesis, Eindhoven, The Netherlands (1985).
7. S. AHMED and F. R. JONES, *Composites* **19** (1988) 4933.
8. *Idem*, *ibid.* **21** (1990) 81.
9. G. M. NEWAZ and W. J. WALSH, *J. Compos. Mater.* **23** (1989) 326.
10. L. L. ANDERSON and R. J. FARRIS, *Polym. Eng. Sci.* **28** (1988) 522.
11. *Idem*, *ibid.* **33** (1993) 1458.
12. *Idem*, *ibid.* **33** (1993) 1466.
13. V. P. VOLODIN, S. K. ZAKHAROV, I. V. KENUNEN, V. I. POMERANTSEV and S. D. SHROGANOVA, *Mech. Compos. Mater.* **30** (1994) 304.
14. YU. P. ZEZIN, *ibid.* **30** (1994) 131.
15. G. RAVICHANDRAN and C. T. LIU, *Int. J. Solids Struct.* **32** (1995) 979.
16. Y. H. ZHAO and G. J. WENG, *Int. J. Damage Mech.* **4** (1995) 196.
17. F. J. GUILD and R. J. YOUNG, *J. Mater. Sci.* **12** (1989) 298.
18. A. V. ZHUK, N. N. KNUNYANTS, V. G. OSHMYAN and V. A. TOPOLKAREA, *J. Mater. Sci.* **28** (1993) 4595.
19. L. E. NIELSEN and R. F. LANDEL, "Mechanical Properties of Polymers and Composites", 2nd Edn (Marcel Dekker, New York, 1994).
20. T. S. CHOW, *J. Polym. Sci.* **16** (1978) 959.
21. J. JANCAR and A. T. DIBENEDETTO, *J. Mater. Sci.* **29** (1994) 4651.
22. I. COLLIAS and D. G. BAIRD, *Polym. Eng. Sci.* **35** (1995) 1167.
23. M. M. BARTENEV and YU. S. ZUYEV, "Strength and Failure of Viscoelastic Materials", 1st Edn (Pergamon Press, London, 1968).
24. I. I. PEREPECHKO, "An Introduction to Polymer Physics", 1st Edn (Mir, Moscow, 1981).
25. R. J. CRAWFORD, "Plastics Engineering", 2nd Edn (Pergamon Press, London, 1987).
26. J. LEMAÎTRE and J. L. CHABOCHE, "Mécanique des matériaux solides", 2nd Edn (Dunod, Paris, 1988).
27. B. FISA, in "Composite Materials Technology Processes and Properties", edited by P. K. Mallick and S. Newman (Hanser, Munich, 1990).
28. L. HOARE and D. HULL, *Polym. Eng. Sci.* **17** (1977) 204.

Received 23 February
and accepted 31 July 1996